Journal of Magnetism and Magnetic Materials 374 (2015) 307–310

Contents lists available at ScienceDirect

Journal of Magnetism and Magnetic Materials

journal homepage: www.elsevier.com/locate/jmmm

Magnetic phase diagram of the low-anisotropy antiferromagnet $Cs_2FeCl_5 \cdot H_2O$

R.S. Freitas *, A. Paduan-Filho, C.C. Becerra

Instituto de Física, Universidade de São Paulo, CP 66318, 05314-970 São Paulo, SP, Brazil

ARTICLE INFO

Article history:
Received 26 July 2014
Received in revised form
14 August 2014
Available online 23 August 2014

Keywords:
Antiferromagnetism
Magnetic phase diagram
Phase transition

ABSTRACT

From magnetization and ac susceptibility measurements we obtain the complete magnetic phase diagram of single crystals of $Cs_2FeCl_5 \cdot H_2O$ for magnetic field up to 15 T. The magnetic field was applied along the directions parallel and perpendicular to the easy axis and the magnetization measured to temperatures down to 0.5 K. At zero magnetic field the antiferromagnetic ordering occurs at $T_N = 6.63$ K. For the field applied parallel to the easy axis the antiferromagnetic (AF) to the spin-flop (SF) transition occurs for fields from 1.4 T to 1.1 T depending on the temperature. The low temperature transition from the (SF) to the paramagnetic (P) phase occurs at 13.15 T. In the perpendicular configuration this transition occurs at fields around 13.5 T. From the extrapolation of the transition fields to zero temperature, we obtain a ratio of the anisotropy field H_A to exchange field H_E, $\alpha = H_A/H_E = (1.4 \pm 0.2) \times 10^{-2}$. A comparison with the phase diagram measured for MnF_2 is included.

1. Introduction

Antiferromagnets of the family $A_2FeCl_5 \cdot H_2O$ (A=K, Rb, Cs) have a very low anisotropy and Néel temperatures ranging from 6.6 K (Cs) to 15 K (K) [1]. Although these systems have been referred and compared to the low anisotropy antiferromagnet MnF_2 ($T_N \approx 67$ K) [2], a complete phase diagram including the phase boundaries to the paramagnetic phase (P) at low temperatures is not available for none of them due to the high fields in which the transition to the P phase occurs. This work is the first to present such a complete phase diagram for one of those systems, namely $Cs_2FeCl_5 \cdot H_2O$ and the mixed compound with a partial substitution of In for Fe.

Previous studies in this system focused on the low field region of the phase diagram ($H < 2.0$ T) [3] and on the specific heat measurements at zero field in the interval $1.5\ \text{K} < T < 30\ \text{K}$ [4]. From these works, that stands as the basic reference on the magnetic and thermal behavior of $Cs_2FeCl_5 \cdot H_2O$, the Néel temperature found is $T_N = 6.57 \pm 0.05$ [2] and the bicritical temperature is $T_B = 6.54 \pm 0.02$ [3]. An anisotropy field $H_A = 0.088$ T and an exchange field $H_E = 7.59$ T given a ratio $\alpha = H_A/H_E = 1.2 \times 10^{-2}$ were obtained from the value of the perpendicular magnetic susceptibility, $\chi_\perp$, in the limit $T \to 0$, and from the extrapolated value of the AF to SF critical field ($H_{AF-SF} = 11.5$ kOe) as the temperature tended to zero [2]. The relevance of the different exchange paths interactions between the Fe sites is discussed in [3], with the conclusion that this system behaves closely to a 3D system with competing interactions. An extensive and detailed report of the weight and relevance of those different exchange paths for the K and Rb analogs compound was given in [5].

When compared to the classical low anisotropy easy axis antiferromagnet MnF_2, which has a rutile structure, the compound $Cs_2FeCl_5 \cdot H_2O$ has a slightly lower anisotropy with a ratio of the anisotropy to the exchange field $\alpha = H_A/H_E \sim 1.2 \times 10^{-2}$ while that found in MnF_2 is $\alpha = 1.6 \times 10^{-2}$ [1,3]. Here we present a complete magnetic phase diagram for $Cs_2FeCl_5 \cdot H_2O$, which allow us to obtain α directly using only the extrapolated critical fields to zero temperature. We anticipate that our results for $H_{AF-SF}(T \to 0) = (1.10 \pm 0.05)$ T and $H_{SF-P}(T \to 0) = (13.15 \pm 0.05)$ T leads to $H_A = (0.092 \pm 0.008)$ T and $H_E = (6.62 \pm 0.03)$ T with a ratio $\alpha = H_A/H_E = (1.4 \pm 0.2) \times 10^{-2}$, which is within the errors expected from previous works [3].

2. Experimental procedures and results

Single crystals of $Cs_2FeCl_5.H_2O$ were grown from aqueous solution of CsCl, $InCl_3$ and $FeCl_3 \cdot 6H_2O$ in the appropriate amounts. These crystals could be carefully oriented with their *a*-axis parallel or perpendicular to direction of the applied magnetic field.

The magnetization and ac susceptibility at low fields were measured with a MPMS (SQUID) system and at high fields with a

* Correspondence to: Universidade de São Paulo, Instituto de Física, Departamento de Física dos Materiais e Mecânica, Rua do Matão, 187 Travessa R, Cidade Universitária, 05508-090 São Paulo, SP, Brazil. Tel.: +55 11 3091 6889.
E-mail address: freitas@if.usp.br (R.S. Freitas).

http://dx.doi.org/10.1016/j.jmmm.2014.08.051
0304-8853/

VSM in a He^3 refrigerator. Sub 2-K ac susceptibility measurements were performed with a susceptometer in a He^3 refrigerator [6]. The transitions point of the phase diagram were obtained either by sweeping the field at a constant temperature or by sweeping the temperature at a constant field and taking the corresponding derivatives *dM/dT* and *dM/dH*.

Fig. 1 shows the magnetization curve obtained at 0.79 K for *H* applied along the easy axis. The step increase of the magnetization at lower fields corresponds to the AF–SF transition and the high field plateau indicates the transition from the SF to the P phase. Above this transition the magnetization saturates as expected. The insert of Fig. 1 shows that some of the field sweeps at temperatures from 1.75 to 6 K from which we mapped AF-SF first order line. The actual locations of these points in the phase diagram were taken from the peak in the derivative of those curves with respect to *H*, *dM/dH*. The magnetic ac susceptibility curves, χ', obtained while sweeping the applied field at fixed values of the temperature are shown in Fig. 2 for a small range of temperature just below the temperature of the bicritical point.

Fig. 3 shows the curves measured at fixed fields by sweeping the temperature for *H* applied along the easy *a*-axis and perpendicular to it. When the magnetic field is applied along the easy axis [Fig. 3(a)] the curves for fields below 1.2 T tend to zero below the

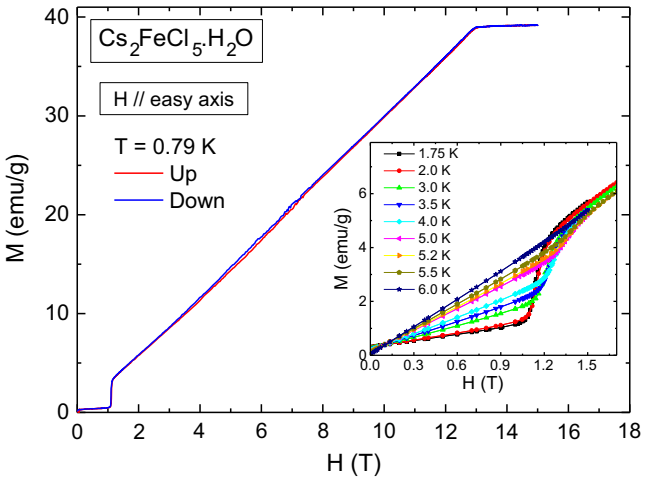

Fig. 1. Magnetization as a function of field at $T=0.79$ K. The inset shows the spin-flop transition at several temperatures.

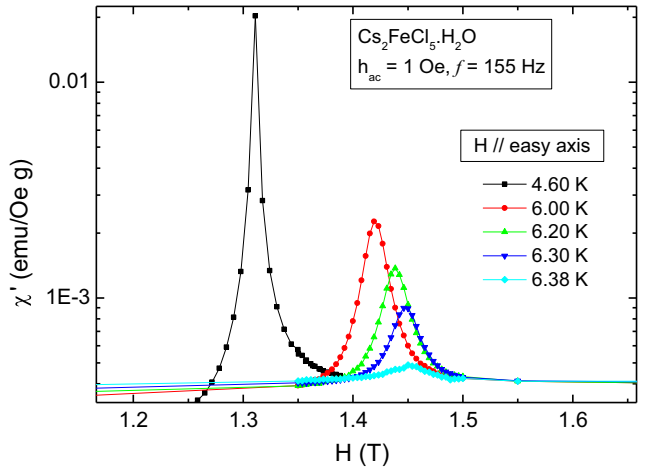

Fig. 2. Magnetic field dependence of the real part of the ac susceptibility for selected temperatures. Data acquired with modulation amplitude $h_{ac}=10$ Oe and modulation frequency $f=155$ Hz.

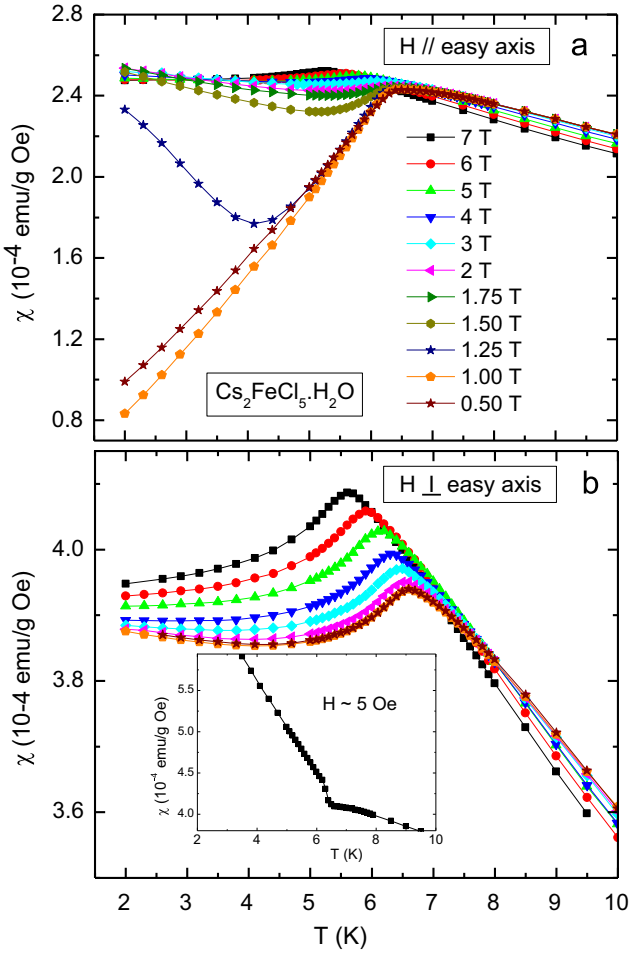

Fig. 3. Temperature dependence of the magnetic susceptibility measured with different magnetic fields applied parallel (a) and perpendicular (b) to the easy axis. The inset shows the dc remanent susceptibility measured in $H\sim5$ Oe.

Néel point when the system enters the AF phase as expected. The gradual rise of the curve measured at 1.25 T indicates that after entering the AF phase around 4 K the AF−SF line is crossed and the susceptibility increases towards its perpendicular value. Above this field the system enters directly from the paramagnetic to the SF phase. For *H* applied perpendicular to the easy axis we observe the expected behavior for this configuration for all values of magnetic fields.

Fig. 4 shows the magnetic phase diagram measured for *H* applied along the easy axis and one of the directions perpendicular to it. The method used to extract the transition points is indicated in the figure.

3. Discussion and conclusion

Close to T_N and at low fields the AF phase boundary to the paramagnetic phase is strongly influenced by the critical fluctuations of the bicritical point since the low anisotropy of this system implies that T_{BP} and T_N are very close and the mean field TH^2 dependence expected for the AF-P boundary is not revealed [7,9].

The Spin Flop phase boundary is a first order transition line and it is weakly dependent on the temperature as usually observed in most antiferromagnetic systems [2,5,7]. This first order transition does not shows any sign of hysteresis and occurs at the thermodynamic transition field H_{AF-SF}, even when some impurities are introduced in the lattice (see below). The explanation for the lack

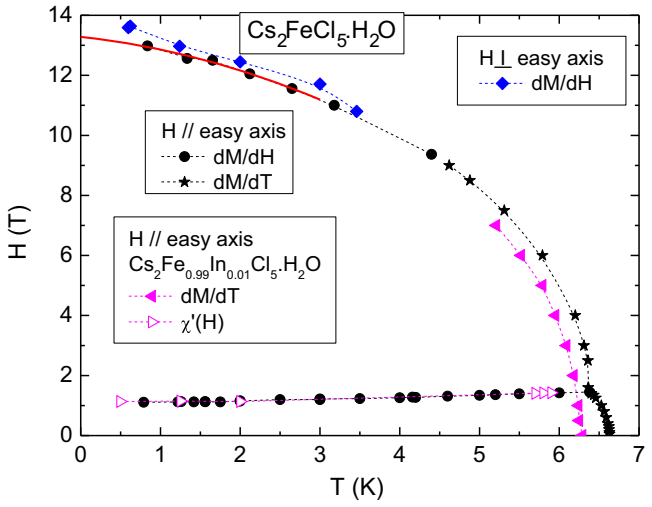

Fig. 4. Phase diagram of $Cs_2FeCl_5.H_2O$ and $Cs_2Fe_{0.99}In_{0.01}Cl_5.H_2O$. The symbols denote the positions of anomalies in the magnetization measured as a function of temperature and magnetic field as indicated in the legend. The red line is a fit to $H=a+bT^2$ as explained in the text. The broken lines are only guide to the eyes. (For interpretation of the references to color in this figure legend, the reader is referred to the web version of this article.)

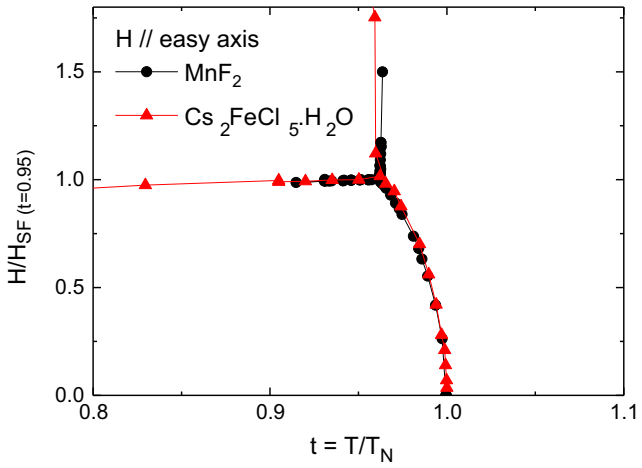

Fig. 5. Phase diagram of MnF_2 and $Cs_2FeCl_5 \cdot H_2O$ in a reduced temperature and field scale as explained in the text.

of hysteresis was given by Keffer and Chow [7]. They showed that it is due to the nucleation of the "incoming" phase either by local imperfections or surface Spin Flop states when the field is increased or by AF local or surface states in decreasing the field. In our case we estimate the extrapolated AF to Spin Flop field when $T\to 0$ is $H_{AF-SF(T\to 0)}=(1.10\pm 0.05)$ T.

The low temperature behavior of the phase boundary from the SF phase to the paramagnetic phase indicates that it is well described by T^2 (solid line in Fig. 4). In fact, due to the mentioned similarities between this compound and MnF_2 we can argue that this temperature dependence is consistent with the behavior found for the phase boundaries in the vicinity of the bicritical point in MnF_2 [8]. For this system it is found that the number of components that became critical is $n=2$, consistent with the orthorhombic anisotropy expected in the plane perpendicular to the easy axis. This also agrees with the spin-wave calculations reported in [9] for the antiferromagnet $NiCl_2 \cdot 4H_2O$, where the terms that account for the orthorhombicity were introduced in the spin Hamiltonian which correspond to the $n=2$ case. A fit with a $T^{3/2}$ law, suitable for uniaxial systems, also give a good fit but with a slightly lower extrapolated $H_{SF-P}(0)$ field. It is expected from the local magnetic ion environment [5] that the in plane (perpendicular to easy axis) anisotropy should be small; thus in the forthcoming analysis we made the option to use the critical field expressions derived for the uniaxial case since they are expressed in terms of H_E and a mean field H_A.

The extrapolated values of the critical field when $T\to 0$ from the T^2 fit are $H_{SF-P}=(13.15\pm 0.05)$ T for H parallel to the easy axis, and $H_{AF-P}\cong(13.5\pm 0.1)$ T for the field applied in the transverse direction. In the limit $T=0$, the second order critical transition fields to the paramagnetic phase can be estimated by the Mean Field Approximation (MFA). When the anisotropy is uniaxial, we find $H_{SF-P}=2H_E-H_A$ when the field is applied along the easy axis, and for the configuration when the external field is applied perpendicular to the easy axis $H_{AF-P}=2H_E+H_A$. These expressions also coincide with the ones obtained from the spin-wave calculations at low temperatures [10]. The corresponding expression as $T\to 0$ for the AF–SF field is $H^2_{AF-SF}=2H_EH_A-H^2_A$. This last expression being also proportional to the gap in the low energy magnon branch of uniaxial antiferromagnets. Using the values of the AF–SF field $H_{AF-SF}(T\to 0)=(1.10\pm 0.05)$ T, and $H_{SF-P}=13.15\pm 0.05$ T leads to an anisotropy field $H_A=(0.092\pm 0.008)$ T and an exchange field $H_E=(6.62\pm 0.03)$ T, with a ratio $\alpha=H_A/H_E=(1.4\pm 0.2)\times 10^{-2}$.

Due to the similarities of this system with MnF_2 [2,8] it is interesting to compare both phase diagrams in a reduced temperature and field scale in the region where equivalent points are present, notably around the bicritical point [8]. We choose $t=T/T_N$ as the reduced scale in temperature and H/H_{SF} with the H_{SF} value at $t=0.95$. This choice of t for the H_{SF} field was made since it corresponds to a temperature with data points available for both compounds in the phase diagram. The data points for MnF_2 were taken from [8]. This plot is shown in Fig. 5. The agreement is quite good and from it the projected field for the SF–P transition in the limit of $t=0$ for MnF_2 is $H_{SF-P}=86$ T.

The inclusion of non-magnetic impurities in this systems leads to the appearance of a remanent magnetization that is observed when a small magnetic field is applied along the easy axis [11]. This behavior is also observed in other low anisotropy antiferromagnets such as MnF_2:Zn [12] and the linear antiferromagnetic chain $(CH_3NH_3)Mn_{1-x}Cd_xCl_3 \cdot 2H_2O$ [13]. Even in the pure compound a very small remanent magnetization has been detected [14]. In our specific case the inclusion of 1% of In ($Cs_2Fe_{0.99}In_{0.01}Cl_5 \cdot H_2O$) results in a decrease in T_N from 6.62 K to 6.29 K and a corresponding shift in the P–AF and P–SP phase boundaries (see Fig. 4). As shown in Fig. 4, no significant change in the AF–SF phase boundary was observed for the doped sample with 1% of In. This contrasts with the hysteretic behavior reported in the K and Rb analogs [15] but these observations were done in samples with much higher concentrations of In ranging from 8% to 15%. It has been suggested that the remament moment is due to a surface effect nucleated either by vacancies (in the pure systems) or by impurities (In), that acts as pinning centers for domain wall formation [13,15]. The low field remanent susceptibility is shown in the inset of Fig. 3(b) and is consistent with that previously measured in this same system [4]. For a 1% concentration of In the increase of the remanent magnetization with respect to that of the pure system is of two orders of magnitude. This magnetization presents a universal behavior that is distinct of the one observed for the antiferromagnetic sub-lattice, as discussed in earlier works where it is suggested that it shows a surface like behavior [4,16].

Acknowledgments

We acknowledge support from FAPESP (07/50968-0) and CNPq (478031/2013-0)-Brazil.

References

[1] R.L. Carlin, F. Palacio, Coord. Chem. Rev. 65 (1985) 141.
[2] Y. Shapira, S. Foner, *Phys. Rev.* B 1 (1970) 3083.
[3] A. Paduan Filho, F. Palacio, R.L. Carlin, J. Physique 39 (1978) L279.
[4] J.A. Puértolas, R. Navarro, F. Palacio, J. Bartolomé, D. González, Richard L. Carlin, Phys. Rev. B 26 (1982) 395.
[5] J. Campo, J. Luzón, F. Palacio, G.J. McIntyre, A. Millán, A.R. Wildes, Phys. Rev. B 78 (2008) 054415.
[6] N.F. Oliveira, A. Paduan-Filho, S.R. Salinas, C.C. Becerra, Phys. Rev. B 18 (1978) 6165.
[7] F. Keffer, H. Chow, Phys. Rev. Lett. 31 (1973) 1061.
[8] Y. Shapira, C.C. Becerra, Phys. Lett. 59A (1976) 75.
[9] C.C. Becerra, N.F. Oliveira Jr, A. Paduan-Filho, W. Figueiredo, W.P. Souza, Phys. Rev. B 38 (1988) 6887.
[10] F.B. Anderson, H.B. Callen, Phys. Rev. 136 (1964) A1068.
[11] A. Paduan-Filho, V.B. Barbeta, C.C. Becerra, M. Gabas, F. Palacio, J. Phys.: Condens. Matter 4 (1992) L607.
[12] T. Fries, Y. Shapira, A. Paduan-Filho, C.C. Becerra, F. Palacio, J. Phys.: Condens. Matter 5 (1993) L107.
[13] A. Paduan-Filho, C.C. Becerra, F. Palacio, Phys. Rev. B 58 (1998) 3197.
[14] Z.V. Carvalho, C.C. Becerra, A. Paduan-Filho, F. Palacio, J. Magn. Magn. Mater 226–230 (2001) 615.
[15] J. Campo, F. Palacio, M.C. Moron, C.C. Becerra, A. Padual-Filho, J. Phys.: Condens. Matter 11 (1999) 4409.
[16] C.C. Becerra, A. Paduan-Filho, T. Fries, Y. Shapira, M. Gabas, J. Campo, F. Palacio, J. Magn. Magn. Mater. 140 (1995) 1475.